International Scientific Journal
Journal of Environmental Science
http://environment.scientific-journal.com/

Experimental and Numerical Prediction of Flow Field around a Panel Radiator

Tamer Calisir[1], Senol Baskaya[1]
Mechanical Engineering Department
Gazi University
Ankara, Turkey
tamercalisir@gazi.edu.tr, baskaya@gazi.edu.tr

Hakan Onur Yazar[2], Sinan Yucedag[2]
R&D Department
DemirDokum A.S.
Bilecik, Turkey
hakanonur.yazar@demirdokum.com.tr

***Abstract*—In this study, the flow field of the heated air above a panel radiator was investigated using particle image velocimetry (PIV) and CFD techniques. Investigations were performed for radiator inlet and outlet water temperatures of 75/65°C. Velocity distribution at different sections above the radiator were observed and it was seen that the velocity distribution changes with the location. It was also observed that a non-symmetrical velocity distribution occurs above the radiator.**

Keywords—Panel radiator; PIV; EN 442-2; Heat transfer

I. INTRODUCTION

Panel radiators are one of the most used heating devices in domestic, business and industrial environments all over the world. Due to rising energy prices and a wish to create environmentally friendly heating systems, there is a demand for a reduction in the total energy consumption. Accordingly, there is an increasing demand for more efficient heating systems. So it is important to increase the efficiency of heating devices such as panel radiators. In the general design of radiators, the heating water is circulated in the hollow radiator and heat is transferred to the cooler surrounding air through the panels and convectors. Most of the heat transferred by the radiators is by natural convection. Hence, it is important to understand the natural convection flow around and inside the radiator, in order to design a more efficient panel radiator.

Different types of radiators have been analyzed by various researchers. Kilic, Sevilgen and Mutlu performed three-dimensional numerical calculations of the thermal output of a steel panel radiator, in accordance with TS EN 442 [1]. Beck, Grinsted, Blakey and Worden considered the enhancement of the heat transfer from panel radiators by the use of either one or two high emissivity sheets placed between the interior surfaces of a double radiator [2]. Müller, Frana, Kotek and Dancova presented the measurement results of the influence of wall temperature on flow from a floor convector. Measurements were realized in an open space laboratory. They visualized the velocity field at the convector inlet and outlet using PIV technique [3]. Laboratory measurements were conducted for radiators with parallel and serial connected panels in an EN 442-2 test room to quantify the possible energy saving of serial radiator by Maivel, Konzelmann and Kurnitski [4]. Myhren and Holmberg performed numerical and experimental studies for radiators and ventilation radiators [5, 6]. In another study, Myhren and Holmberg focused in their investigation how different heating systems and their position affect the indoor climate in an exhaust-ventilated office under Swedish winter conditions [7]. Peukert and Müller described measurements based on mass flow and temperature of floor convectors in cooling and heating regimes. Particle trace method was used for the visualization of the flow inside and outside the convector [8]. The utility of a stoneware panel covering radiators to improve their energy performance was analyzed using theoretical and experimental methods by Diaz, Galan, Rodriguez and Calleja [9]. Erdogmus conducted experimental studies in a standard test room to determine heat outputs of radiators. The heat dissipation capabilities of three different panel radiators were also determined using numerical methods [10]. Aydar and Ekmekci performed CFD analysis of existing panel radiators with a commercial CFD code with a variable connection method in three dimensional space [11].

The airflow field in a room and the natural convection flow in closed was also investigated and some studies are presented in this study. Cao, Liu, Jiang and Chen firstly gave an introduction of the typical PIV technologies used in indoor environment measurement, and then summarized the applications of PIV in measuring in the indoor airflow fields [12]. Corvaro, Paroncini and Sotte performed an analysis of natural convection in an enclosure filled with air and with opposite heated and cooled walls is performed for four different tilt angles using PIV and numerical techniques [13]. In another study, Corvaro and Paroncini provided an experimental analysis of the natural convection in a differentially heated square enclosure using 2D-PIV [14]. Velocity measurements of natural convection in symmetrically heated vertical channel using PIV system was performed by Ayinde, Said and Habib [15]. Posner, Buchanan and Dunn-Rankin compared CFD results with laser Doppler anemometry (LDA) and particle image velocimetry (PIV) measurements of air flow in an isothermal model room [16]. The application of PIV and CFD techniques to measure the velocity field inside the air cavity of an open joint ventilated facades model was investigated in [17, 18].

As can be seen, from the literature review there have been some studies about panel radiators and PIV measurement of natural convection flows. However, there is a lack in the literature in the measurement of air flow field around panel radiators. It is important to observe the flow of the heated air at

the top of the radiator. So, the main goal of this study is to observe the flow field around a panel radiator presently manufactured, using numerical methods and particle image velocimetry (PIV) measurement technique. The aim was to predict the velocity and flow field of the heated air over a PCCP (panel-convector-convector-panel) radiator. These findings are important and will serve in the study to design a new panel radiator with a higher heat output. Experiments were performed for a panel radiator with the dimensions of 600x1000 mm under controlled laboratory conditions with a room temperature of 20°C. Same conditions were implemented in the FloEFD CFD code. Experiments and simulations were performed for a water inlet and outlet temperature of 75°C and 65°C, respectively. These temperatures were selected according to the EN 442-2 standard [19]. PIV measurements were performed at different sections along the radiator, and the flow field was observed at the upper sections of the radiator. Hence, the air velocity which flows through the convectors and leaves at the upper section of the radiator was obtained.

II. Experimental Setup

In this part of the study the experimental setup is described. The experimental setup is shown in Fig. 1. Experiments were performed in a test room where temperature conditions can be stable and the temperature of 20 °C was used as the temperature of the test room. This temperature was selected according to EN 442-2 standard [19]. The radiator thermal performance test rig consists of a 1000 mm × 600 mm radiator, constant temperature water bath, a circulation pump, immersion type thermocouples to measure water temperatures at the inlet and outlet of the radiator, thermocouples to track the room temperature, a Coriolis mass flow meter, a computer connected data logger for tracking the temperatures of the room and radiator inlet and outlet ports, and necessary piping. Experiments were performed for an inlet water temperature of 75°C and outlet water temperature of 65°C. According to EN 442-2 standard experiments were performed for a water inlet location at the top side of the radiator and outlet section at the same side at the bottom. As can be seen from Fig. 1, the heating water was heated in a constant temperature water bath (LABO H541-D23) to the desired temperature, and was circulated using a pump through the piping. The flow rate was measured using a Kobold TME S80 Coriolis mass flow meter, and the desired flow rate was adjusted using a by-pass connection and a needle valve. The mass flow meter was mounted at the outlet side of the radiator. Also, at the return line the circulation water was filtered using two different filters. At the inlet and outlet ports of the radiator, two at each, immersion type thermocouples were used. Temperature values were obtained using Agilent 34970 A model data logger. These were tracked using the BenchLink Datalogger 3 software. A DemirDöküm Panel Plus radiator with a dimension of 1000 mm x 600 mm was used in the performance tests. The distance between the nearest heat emitting surface of the radiator and the outer wall is 0.05 m. Tested radiator is positioned at a height of 0.11 m above the floor according to EN 442-2. The room temperature was hold at 20°C using an air conditioner and was tracked during the experiments. These were placed according to EN 442-2 [19]. At the center of the room at vertical heights of 0.05 m, 0.75 m, and 1.50 m from the bottom, and 0.05 m from the ceiling thermocouples were used to measure the room temperature.

The inside and outside of the test room are presented in Fig. 2. As can be seen from the figure the radiator and the wall with the radiator mounted were painted with a black low-reflection paint.

A CCD camera (FlowSense) with a 60 mm Nikkor lens covered with a green filter (532 nm wavelength) was used for image capturing. The image resolution was 1600x1200 pixels; the effective measured field was about 1000x1000 pixels. For the illumination of the measurement plane a Nd:YAG laser with a wavelength of 532 nm and power of 120 mJ was employed. The laser head was mounted on a light guiding arm to easily move the laser sheet to the measurement section. There is a cylindrical lens at the outlet section of the laser head, which transforms the laser to a planar light sheet. The laser and the camera were controlled by a computer. The flow field was processed using DynamicStudio v3.31 which was produced by Dantec Dynamics [20]. The signals were processed with a technique which is based on the cross-correlation function, using a Fast Fourier Transform. The size of the interrogation areas were 32 x 32 pixels. An overlap of 50% was used in the horizontal and vertical directions. The adaptive correlation method was used for the evaluation of the vector field and afterwards a moving-average validation method was used to accept and reject vectors from the vector field.

The heat output is calculated from temperature data collected under steady state test room conditions, using inlet-outlet temperature values. Therefore, the main consideration in the measurements is that whether or not all the temperatures reach the steady state condition. The steady state condition was followed with controlling the temperature values. After the steady state conditions were obtained, approximately after 3 hours, measurements were started, and all tests were continued for one hour. However, in this study only flow field results over the panel radiator are presented.

A. PIV measuring procedure

During the experiments, temperature values were obtained every 10 seconds. Using the PIV technique every 5 min 200 image couples were acquired and analysed. This was done to control the repeatability of the measurements and also the signal-to-noise ratio were checked after the measurements.

Experiments were performed for an inlet water temperature of 75°C and outlet water temperature of 65°C. According to EN 442-2 standard experiments were performed for a water inlet location at the top side of the radiator and outlet section at the same side at the bottom.

Measurements were performed at different sections above the radiator. The locations are shown on Fig. 3. Also the circulation water inlet side was presented on the figure. Due to the water distribution in the water channels of the radiator a non-uniform temperature distribution on the panels was seen in the literature [1, 10, 11]. Hence, it is expected that the velocity values and flow field will change from section to section.

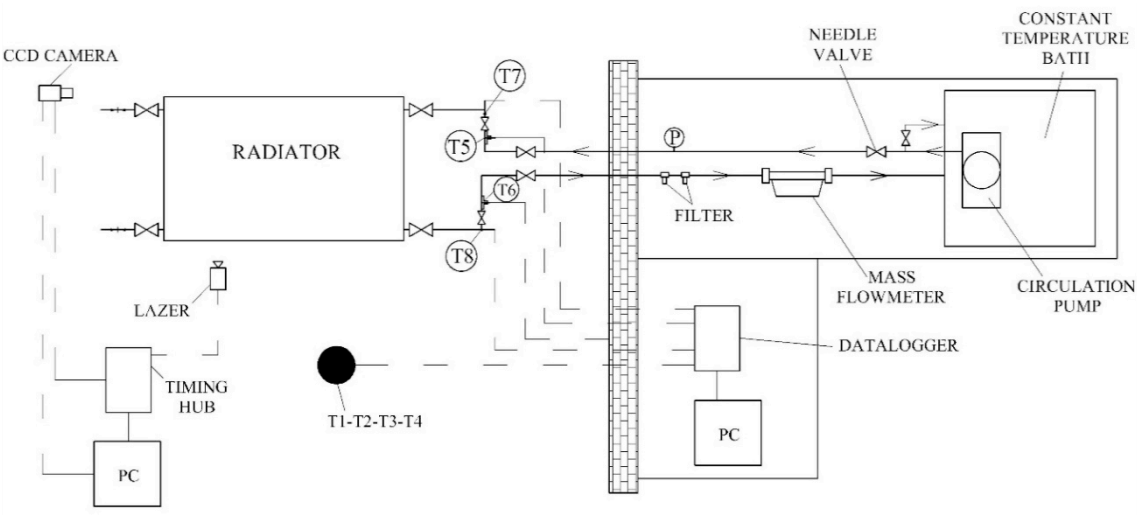

Fig. 1. Experimental Setup

PIV is a non-intrusive measurement method, so the natural convection flow over and around the radiator was not affected by the laser. The trigger rate was set as 10 Hz and different times between pulses were tried, and the optimum time between pulses were found as 1000 μs.

Acid-Ester was used as tracer particles and the fluid was seeded into the flow using an atomizer. The atomizer generates seeding particles that have a diameter of approximately 1μm. Fig. 4 shows the seeding density inside the experimental space over the radiator.

(a)

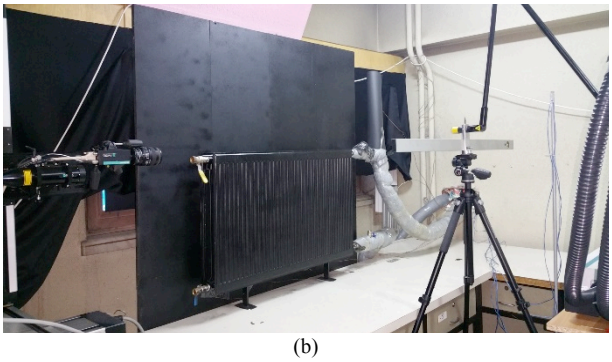

(b)

Fig. 2. Test room (a) Outside of the test room, (b) Inside of the test room

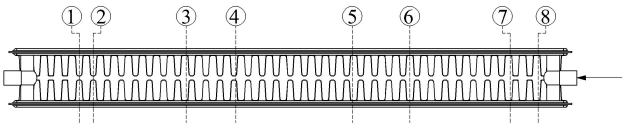

Fig. 3. Velocity Measurement Locations over the Panel

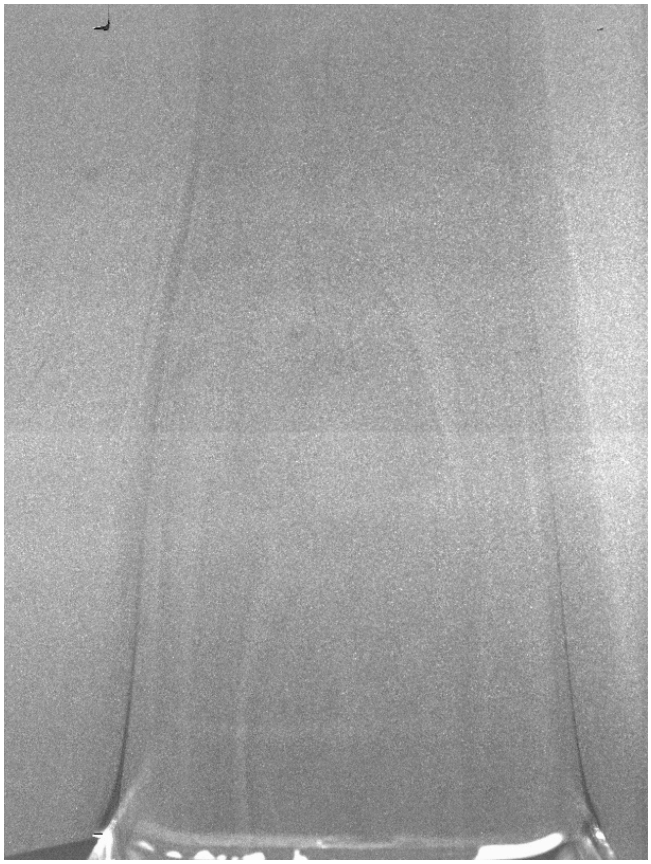

Fig. 4. Seeding density

III. NUMERICAL MODEL

The numerical model employed in this study is presented in this part. Also, the specified boundary conditions and governing equation are shown. The FloEFD CFD code was used in this study. The room geometry with the radiator is shown in Fig. 5. This geometry was used as the computational domain. The room was modelled with the dimensions of 4 m x 4 m x 3 m in the x-y-z directions, respectively. These dimensions were selected according to EN 442-2 [19]. The opposite side of the radiator was modeled as outlet to remove the heated air and get fresh air again from this outlet. Hence, it was possible to achieve a 20°C room temperature.

There exists two different fluids in the model. The circulation water which flows through the hollow radiator channels transfer its heat to the steel radiator walls. The heat is conducted through the radiator walls and was transferred through natural convection and radiation to the air and walls of the room. The used radiator geometry is shown in Fig. 6, and the steel properties of the radiator are presented in Table I.

The boundary conditions implemented in the numerical model are shown on Fig. 7. An inlet and outlet was defined for the circulation water in the radiator. The connection pipes were perfectly insulated. Also, the wall where the radiator is mounted was modeled as perfectly insulated. A constant temperature of 20°C was defined to the remaining walls. In the negative z direction, a gravity of 9,81 m/s^2 was implemented. Emissivity of the room walls and panels of the radiator were given as 0.9 and 0.88, respectively. The discrete transfer radiation model was chosen in the model. It was seen that the effect of radiation is in the range of 25-30% so the radiation heat transfer was added to the model.

The calculated Re number in accordance to the water inlet channel was found to be 7000, so the flow was considered as turbulent. The Grashof number on the panel radiator was calculated as approximately Gr<10^9. However, the air flow in the room was considered as turbulent. So, the water flow as well as the air flow in the room was taken as turbulent, and the k-ε turbulence model was implemented in the numerical model.

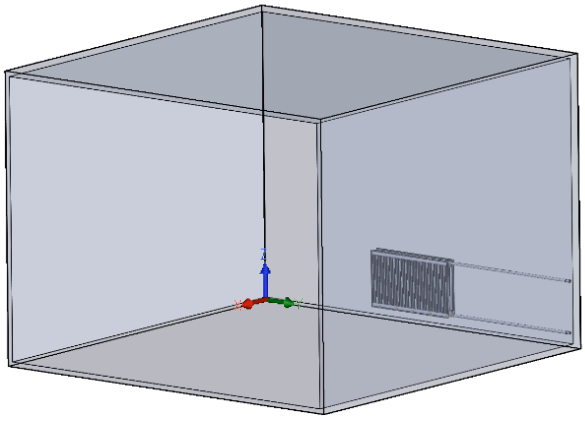

Fig. 5. Room and radiator location

TABLE I. PROPERTIES OF STEEL

Property	Values
Density (kg/m^3)	7850
Conductivity (W/m.K)	19.9
Specific heat (J/kg.K)	450

The Reynolds and Grashof numbers were calculated as follows;

$$Re = 4.\dot{m} / \mu.\pi.D \quad (1)$$

$$Gr = g.\beta.(T_s - T_\infty).L^3 / \nu^2 \quad (2)$$

where, m (kg/s) shows the mass flow rate, μ (Pa.s) the dynamic viscosity of water and D (m) the diameter of the water inlet channel. L (m) shows the panel height, g the gravity (m/s^2), T_s (°C) surface temperature of the panel, T_∞ (°C) air temperature, ν (m^2/s) kinematic viscosity of air. The expansion coefficient (β) was predicted as follows;

$$\beta = 1 / T_f \quad (3)$$

where, T_f shows the film temperature of air and was calculated with the equation given below.

$$T_f = (T_s + T_\infty)/2 \quad (4)$$

The heat output of the radiator was calculated according to EN 442-2 [19].

$$Q = \dot{m}.(h_i - h_o) \quad (5)$$

Inlet and outlet enthalpies of water are shown as h_i (J/kg) and h_o (J/kg), respectively. These were evaluated according to the inlet and outlet temperatures of water using thermodynamic tables [21].

The numerical code was firstly verified and the convergence was investigated. These were checked, and it was seen that the simulation becomes almost independent after 300 iterations. An ideal mesh number was selected as 465.484 cells. The mesh was refined near the radiator and around the convectors.

Finally, the numerical results were compared with experimental results. Table II shows the experimental and numerical comparison. The numerical results are in agreement with the experimental results.

TABLE II. EXPERIMENTAL AND NUMERICAL RESULTS

Q (W) – Num.	Q (W) – Exp.	Difference (%)
1781.67	1800.25	1.03

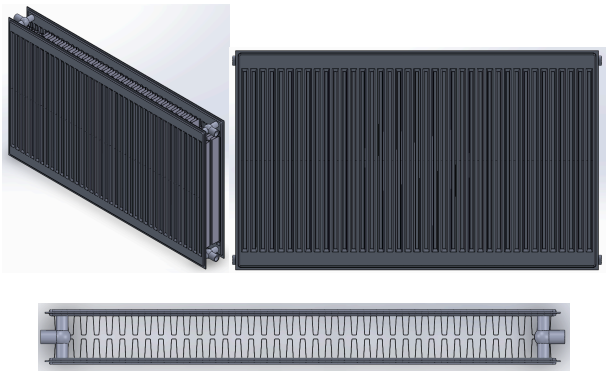

Fig. 6. Panel radiator geometry

The CFD code was also verified with the PIV measurement results. Fig. 8 shows the velocity values 20 mm above the radiator obtained by PIV and CFD. These values were acquired at Location 1 and Location 4. Although, it was observed that the CFD results over predicted the velocity values at some locations. But in general one can see that the CFD results are in agreement with the PIV measurements. Also, the locations which were not shown here are in good agreement with the experimental PIV results.

A. Governing equations and Boundary conditions

The governing equations used in the simulation of the three-dimensional, steady, turbulent, incompressible problem are shown in this part of the study. As mentioned before, the flow in the water channels is forced convection. The circulation water transfers its heat through conduction to the environmental air. The air near the radiator is heated and the density of air falls and it begins to rise. As can be seen, all types of heat transfer occur on a radiator. Therefore, the governing equations and boundary conditions for air and water were presented separately.

The natural convection air flow was modeled using the Boussinesq approximation. The k-ε turbulence model was employed for the solution of the turbulent quantities. The air, inside the room was accepted to not affect the radiation and the Discrete Transfer model was employed to solve the radiation effects.

The three-dimensional turbulent mass, momentum and energy conservation equations for forced convection flow of water is given as follows,

$$\frac{\partial U_i}{\partial x_i} = 0 \tag{6}$$

$$\rho U_i \frac{\partial U_j}{\partial x_i} = -\frac{\partial P}{\partial x_j} + \frac{\partial}{\partial x_i}\left[\mu\left(\frac{\partial U_i}{\partial x_j} + \frac{\partial U_j}{\partial x_i}\right) - \rho\overline{u_i' u_j'}\right] \tag{7}$$

$$\rho c_p U_i \frac{\partial T}{\partial x_i} = \frac{\partial}{\partial x_i}\left[k\frac{\partial T}{\partial x_i} - \rho c_p \overline{u_i' T'}\right] \tag{8}$$

Conjugate heat transfer exists at the panel walls of the radiator. The following boundary condition exists at the water side of the panel;

$$k_{panel}\left(\frac{\partial T}{\partial n}\right)_{panel} = k_{water}\left(\frac{\partial T}{\partial n}\right)_{water} \tag{9}$$

where k shows the heat conduction coefficient and n the normal of the surface.

The turbulent mass, momentum and energy conservation equations for air in the computational domain are shown below. As shown in Fig. 7 all walls of the room were modeled as 20°C, except the wall where the radiator was mounted. This wall was modeled as perfectly insulated. Thus, the temperature gradient at this wall is zero. The opposite side of the panel radiator was modeled as outlet to the atmosphere at 20°C, so the heated air left the room and fresh air entered the room. At all walls, panel and convector surfaces the velocity was zero, due to the non-slip wall boundary condition.

$$\frac{\partial U_i}{\partial x_i} = 0 \tag{10}$$

$$\rho U_i \frac{\partial U_j}{\partial x_i} = -\frac{\partial P}{\partial x_j} + \frac{\partial}{\partial x_i}\left[\mu\left(\frac{\partial U_i}{\partial x_j} + \frac{\partial U_j}{\partial x_i}\right) - \rho\overline{u_i' u_j'}\right] - g_i\beta\left(T - T_\infty\right) \tag{11}$$

$$\rho c_p U_i \frac{\partial T}{\partial x_i} = \frac{\partial}{\partial x_i}\left[k\frac{\partial T}{\partial x_i} - \rho c_p \overline{u_i' T'}\right] \tag{12}$$

Conjugate heat transfer occurs at the panel and convector surfaces. The wall boundary condition at the mentioned surfaces could be described as follows;

$$-k_{panel}\left(\frac{\partial T}{\partial n}\right)_{panel} = -k_{air}\left(\frac{\partial T}{\partial n}\right)_{air} + q_{rad} \tag{13}$$

where, q_{rad} shows the radiation heat transfer from the panel and convectors.

The k-ε turbulence model was implemented in the code to solve the turbulence quantities. The equations which characterize these model are as follows;

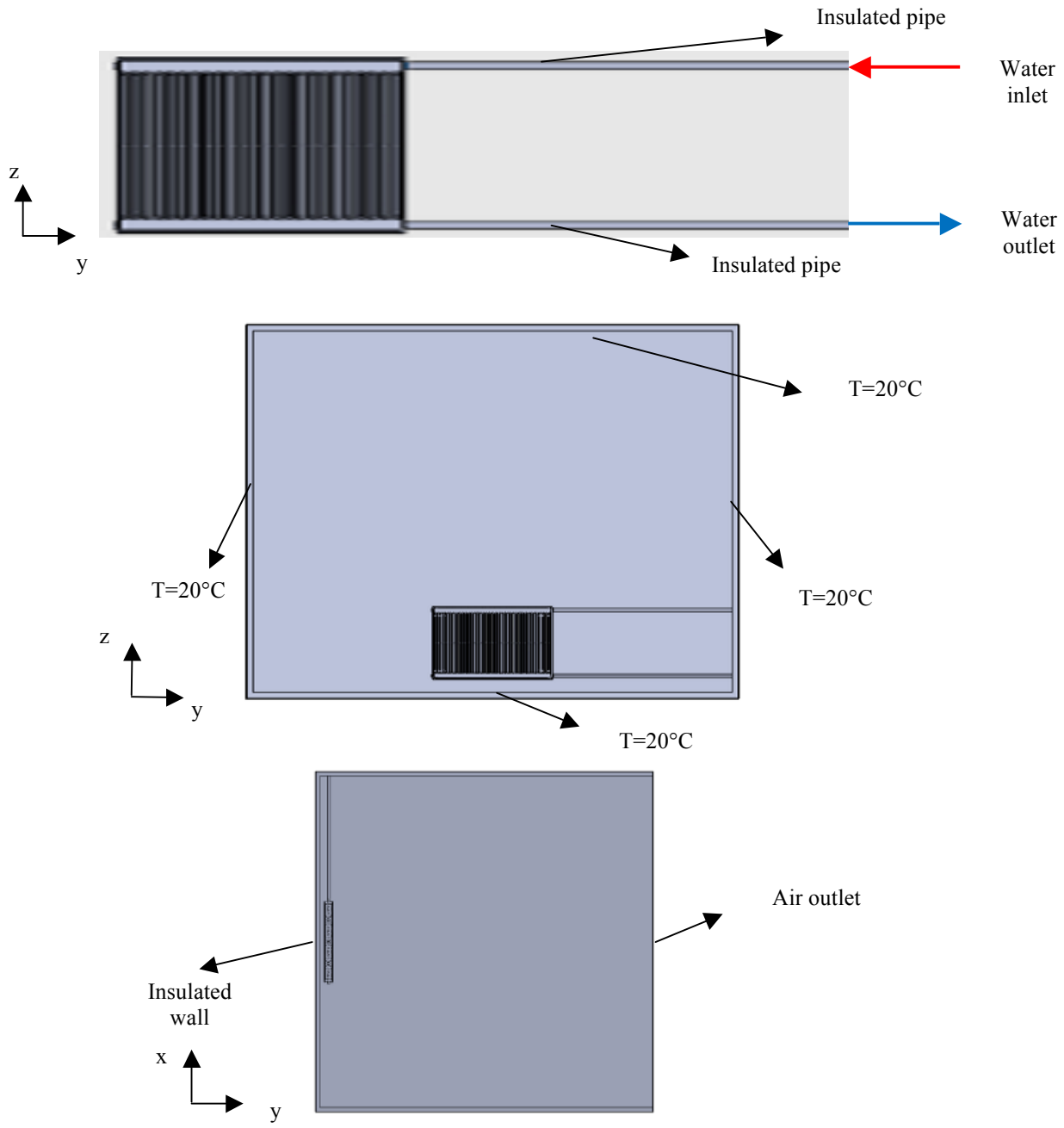

Fig. 7. Boundary conditions

$$\rho U_i \frac{\partial k}{\partial x_i} = \frac{\partial}{\partial x_i}\left[\left(\mu + \frac{\mu_t}{\sigma_k}\right)\frac{\partial k}{\partial x_i}\right] + \mu_t\left(\frac{\partial U_i}{\partial x_j} + \frac{\partial U_j}{\partial x_i}\right)\frac{\partial U_i}{\partial x_j} - \rho\varepsilon \quad (14)$$

$$\rho U_i \frac{\partial \varepsilon}{\partial x_i} = \frac{\partial}{\partial x_i}\left[\left(\mu + \frac{\mu_t}{\sigma_\varepsilon}\right)\frac{\partial \varepsilon}{\partial x_i}\right] + f_1 C_1 \mu_t \frac{\varepsilon}{k}\left(\frac{\partial U_i}{\partial x_j} + \frac{\partial U_j}{\partial x_i}\right)\frac{\partial U_i}{\partial x_j} - f_2 C_2 \rho \frac{\varepsilon^2}{k} \quad (15)$$

The turbulence kinetic viscosity is given below;

$$\mu_t = f_\mu C_\mu \rho \frac{k^2}{\varepsilon} \tag{16}$$

The wall damping functions are unity for the standard model. $C_{1\varepsilon}$, $C_{2\varepsilon}$ and C_μ are constant coefficients of the k-ε model. In addition, σ_k ve σ_ε are the turbulent Prandtl numbers of k and ε, respectively. Experimental coefficients used in the equations are given below.

$$\sigma_k = 1{,}00; \quad \sigma_\varepsilon = 1{,}314; \quad C_1 = 1{,}44; \quad C_2 = 1{,}92; \quad C_\mu = 0{,}09 \tag{17}$$

IV. Results and Discussion

The results obtained from the PIV measurements and CFD study are shown in this part of the study. The presented results were obtained for an inlet and outlet water temperature of 75/65°C. Measurements were performed above the radiator to observe the velocity and flow field of heated air above the radiator. The heated air leaves the radiator which could be described as a flow between two plates. The flow between the panels of the radiator could not be observed due to optical access limitations. However, these values were obtained by CFD at different heights and shown in this section.

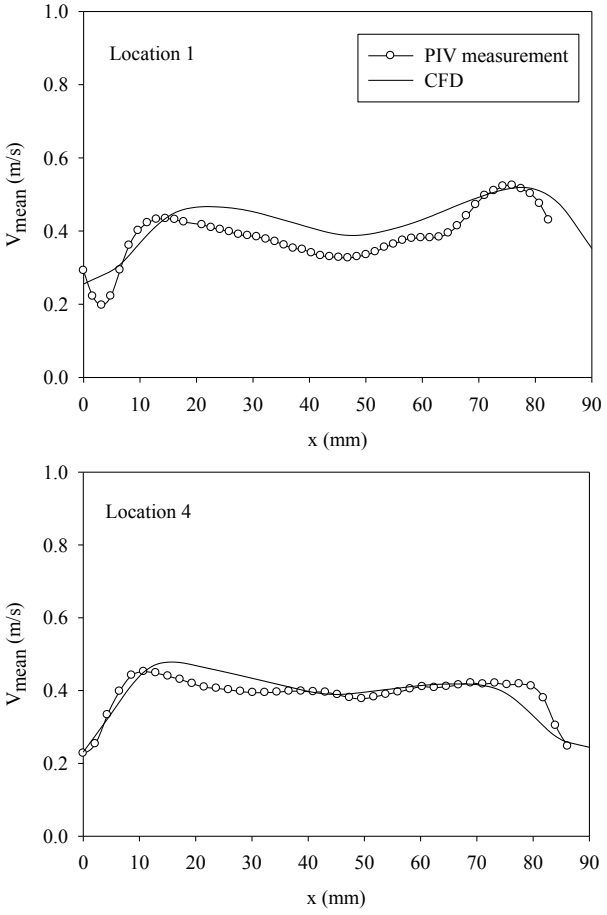

Fig. 8. Comparison of PIV and CFD results

Fig. 9. shows the velocity distribution at different measurement locations. The values were obtained 20 mm above the radiator. Temperature measurements of the heated air were also performed above the radiator at this heigth. So, the velocities along the width of the radiator are shown on the figure. As can be seen, the velocity distribution changes along the radiator. This is due to the different temperature distributions of the panel which directly effects the velocity distribution and values. Another important observation is that the velocity distribution is not symmetrical considering the mid between the two panels of the radiator as symmetry line. This is due to the non-symmetrical temperature distribution at both sides of the panel radiator. One of the panels faces the insulated wall, where the other one faces the room. Hence, due to the non-symmetrical temperature distribution the velocity develops non-symmetrical. This could be better observed in Fig. 10. Velocity contours and vectors are presented in Fig. 10. at different locations. One can see that there exists a non-symmetrical flow above the radiator. The right side of the figures represent the radiator panel side which faces the room, where the left side faces the insulated wall, where the radiator is connected. However for Location 1 and Location 2 there exists almost a symmetrical distribution of the velocity field above the radiator. The rising heated air moves almost linearly and changes almost no direction above the radiator for these two mentioned locations.

The flow changes its direction for Location 3 – Location 8. An almost stagnant region is observed at the right of the figure, and the flow changes its direction to the wall where the radiator is mounted. From the streamline distribution presented in Fig. 11. it can be seen that the air on the right side moves to main stream and the flow moves to the wall. CFD results, which are not presented in this study showed that the flow merges with the wall at a certain height, and moves along the wall until it reaches the ceiling of the test room.

The flow between the two panels of the panel radiator and convectors is also important. However, due to optical access it was not possible to measure this field using PIV. Due to this, CFD results were used to observe the velocity distribution between the panels, and this has been shown on Fig. 12.

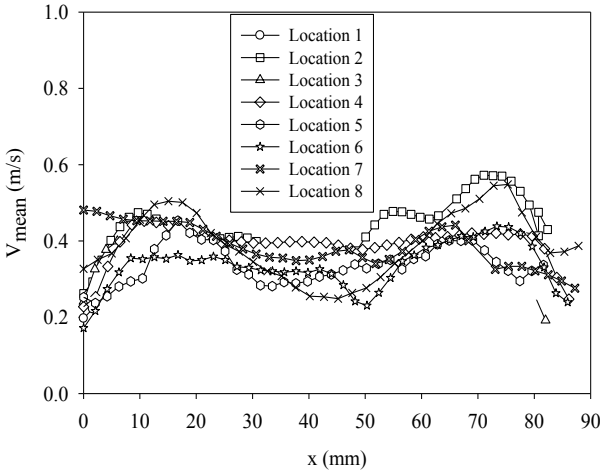

Fig. 9. PIV measurement results at different locations

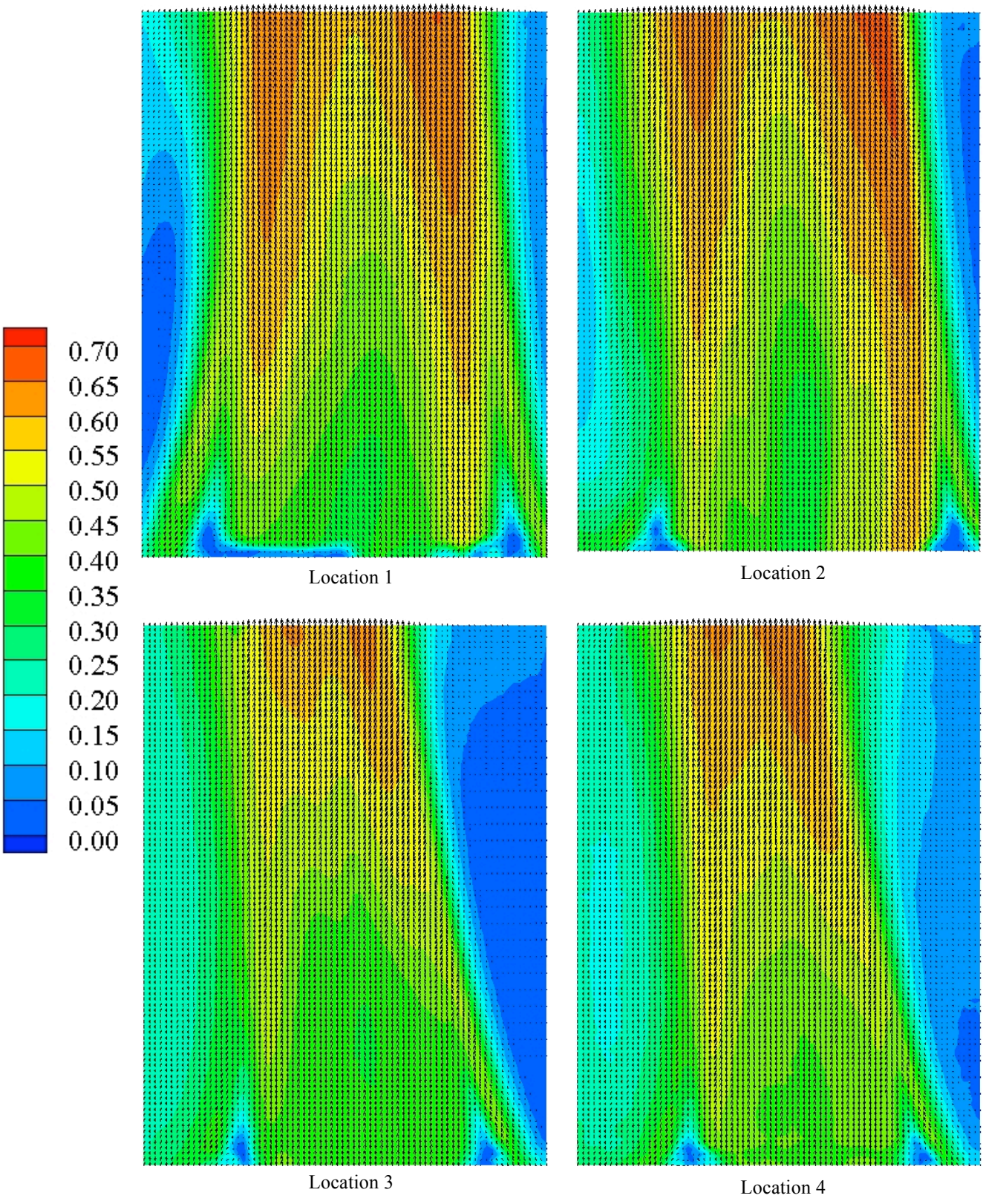

Fig. 10. Velocity contours and vectors at different measurement locations above the radiator

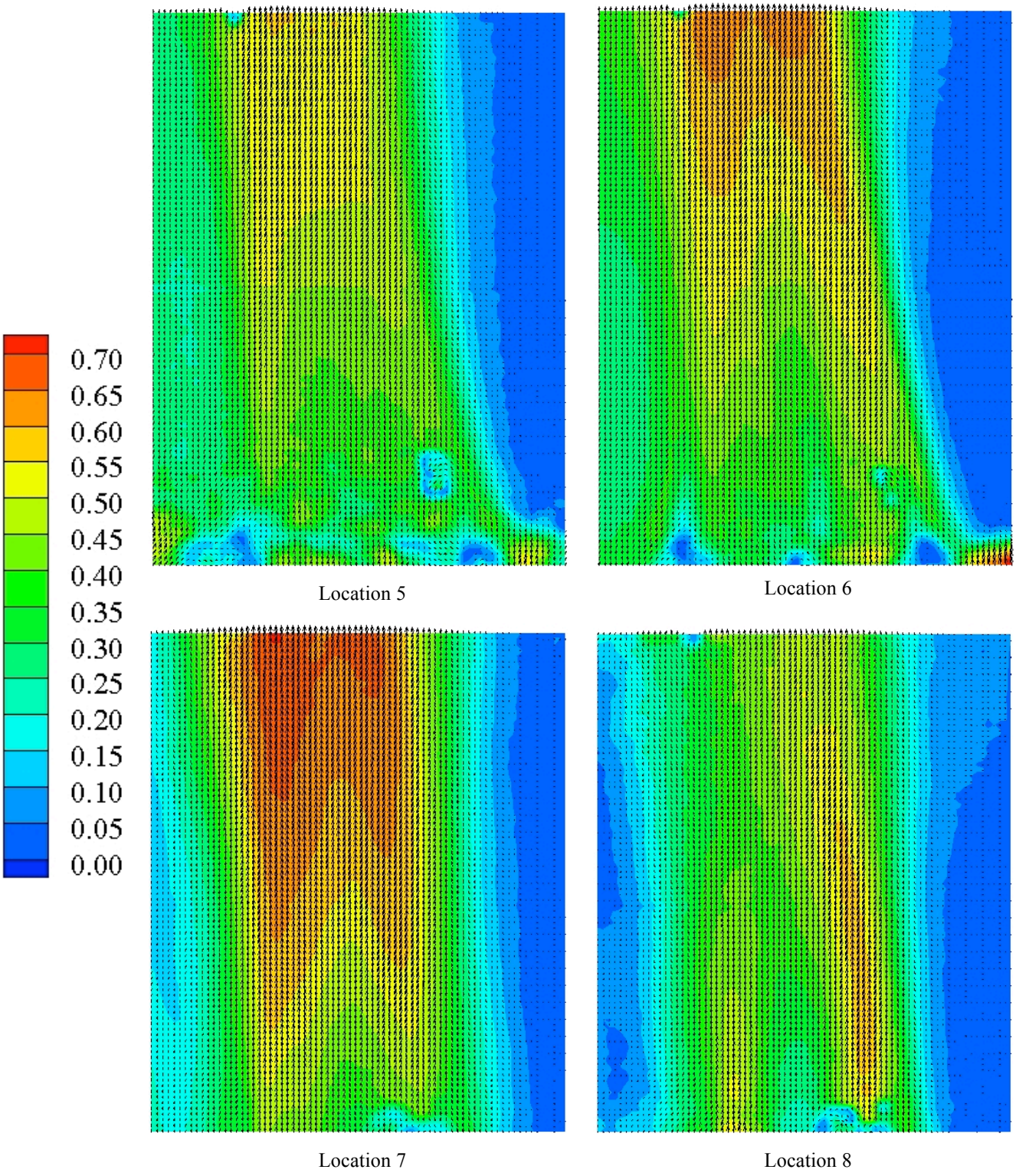

Fig. 10. Velocity contours and vectors at different measurement locations above the radiator (continued)

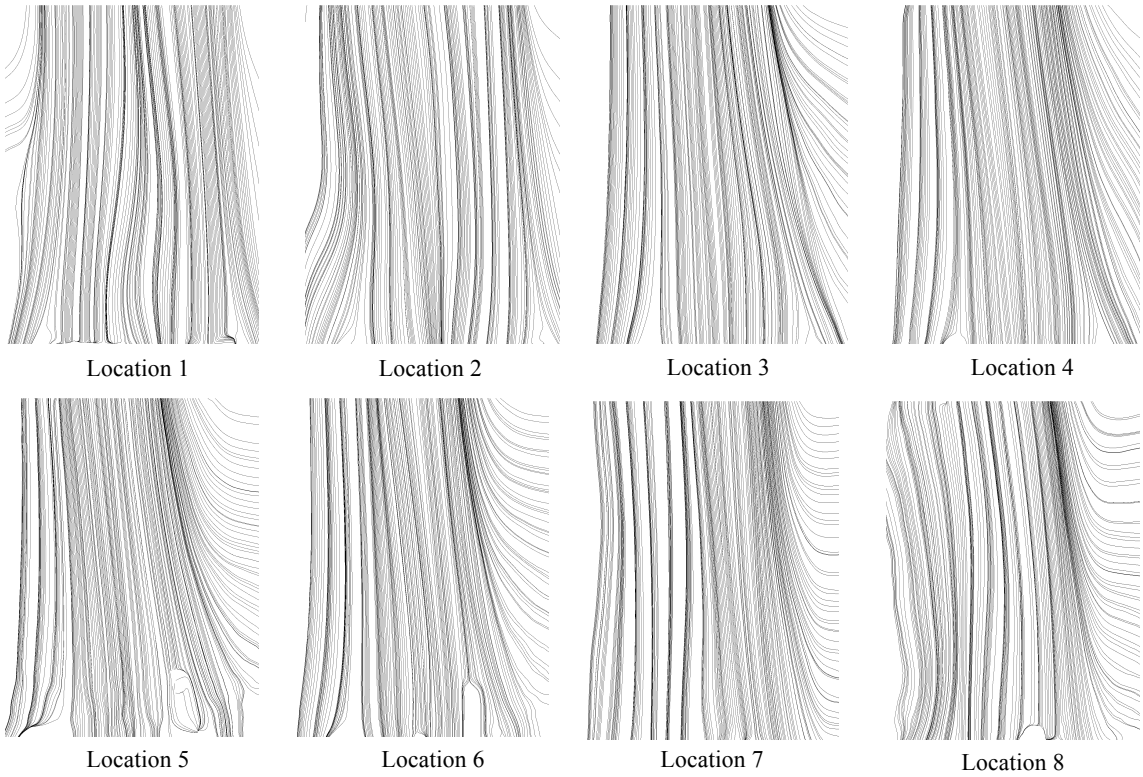

Fig. 11. Streamlines at different locations

Location 1 and Location 4 are regions where the convectors have a height of 0.51 m. However, the first three convectors at both ends of the radiator are shorter and Location 8 is the location at a shorter convector.

In the Fig. 12. z=0 m represents the low side of the radiator and z=0.6 m shows the upper end of the radiator. As can be seen from the figures, velocity distributions for Location 1 and Location 4 are very similar. However, due to higher temperature distributions at Location 4 (observed before) higher velocity values were obtained, especially around the convector tips (x=0.037m – 0.044m).

Contrary to Location 1 and Location 4 the velocity at the convector tips is non-zero at the heights of z=0.2 m and z=0.4 m.

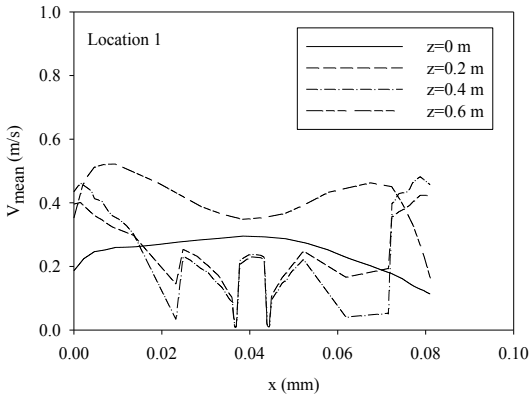

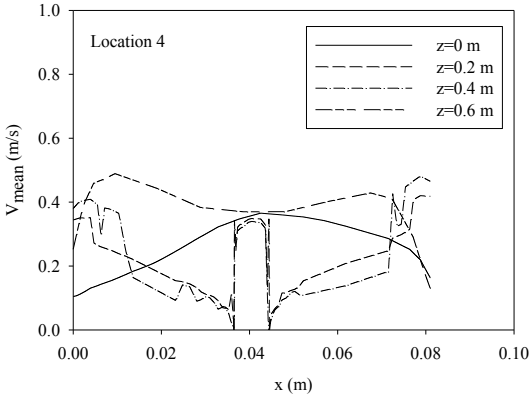

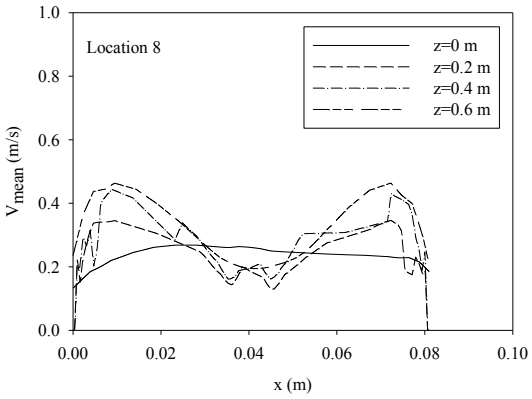

Fig. 12. Mean velocities at different heights of the panel radiator.

V. CONCLUSION

The flow field of the heated air above a panel radiator was investigated using particle image velocimetry (PIV) and CFD techniques. Investigations were performed for radiator inlet and outlet water temperatures of 75/65°C. Experiments were performed for a panel radiator with the dimensions of 600x1000 mm under controlled laboratory conditions with a room temperature of 20°C. Same conditions were implemented in the CFD code. The aim was to predict the velocity and flow field of the heated air above a PCCP (panel-convector-convector-panel) radiator.

Velocity distributions at different sections above the radiator were observed, and it was seen that the velocity distribution changes with location. It was observed that the velocity distribution changes along the radiator, which is due to the different temperature distributions of the panel, which directly effects the velocity distributions. Another important observation was that the velocity distribution is not symmetrical considering the mid between the two panels of the radiator as symmetry line.

The findings of this study are important and will serve in the study to design a new panel radiator with a higher heat output. Hereafter, it will be possible to use lower circulation water temperatures in daily use, reducing fossil fuel consumption.

ACKNOWLEDGMENT

The financial support of this study by the Ministry of Science, Industry and Technology of Turkey under Grant number 0641.STZ.2014 and also DemirDöküm A.Ş. are gratefully acknowledged.

REFERENCES

[1] M. Kilic, G. Sevilgen, and M. Mutlu, "Three-Dimensional Numerical Analysis of Thermal Output of a Steel Panel Radiator," Exergy, Energy, and the Environment, 1st ed., Chapter 55, pp. 585-593, 2014.

[2] S.M.B. Beck, S.C. Grinsted, S.G. Blakey, K. Worden, "A novel design for panel radiators," Applied Thermal Engineering, vol. 24, pp. 1291-1300, 2004.

[3] M. Muller, K. Frana, M. Kotek, P. Dancova, "The influence of the wall temperature on the flow from the floor convector (experimental results)," EPJ Web of Conferences, vol. 45, pp. 01130, 2013.

[4] M. Maivel, M. Konzelmann, J. Kurnitski, "Energy performance of radiators with parallel and serial connected panels," Energy and Buildings, vol. 86, pp. 745-753, 2015.

[5] J.A. Myhren, S. Holmberg, "Design considerations with ventilation-radiators: Comparisons to traditional two-panel radiators," Energy and Buildings, vol. 41, pp. 92-100, 2009.

[6] J.A. Myhren, S. Holmberg, "Performance evaluation of ventilation radiators," Applied Thermal Engineering, vol. 51, pp. 315-324, 2013.

[7] J.A. Myhren, S. Holmberg, "Flow patterns and thermal comfort in a room with panel, floor and wall heating," Energy and Buildings, vol 40, pp. 524-536, 2008.

[8] P. Peukert, M. Müller, "Measurement of Floor Convectors at Special Laboratory and First Results," EPJ Web of Conferences, vol. 25, pp. 01071, 2012.

[9] A. Menendez-Diaz, C. Ordonez-Galan, J.B. Bouza-Rodriguez, J.J. Fernandez-Calleja, "Thermal analysis of a stoneware panel covering radiators," Applied Energy, vol. 131, pp. 248-256, 2014.

[10] A.B. Erdogmus, Simulation of the Heater Test Room Defined by EN 442 Standard and Virtual Testing of Different Type of Heaters. PhD. Thesis, Izmir: Izmir Institute of Technology, 2011.

[11] E. Aydar, I. Ekmekci, "Thermal Efficiency Estimation of the Panel Type Radiators with CFD Analysis," J. of Thermal Science and Technology, vol. 32, No. 2, pp. 63-71, 2012.

[12] X. Cao, J. Liu, N. Jiang, Q. Chen, "Particle Image Velocimetry measurement of indoor airflow field: A review of the technologies and applications, "Energy and Buildings, vol. 69, pp. 367-380, 2014.

[13] F. Corvaro, M. Paroncini, M. Sotte, "PIV and numerical analysis of natural convection in tilted enclosures filled with air and with opposite active walls," International Journal of Heat and Mass Transfer, vol. 55, pp. 6349-6362, 2012.

[14] F. Corvaro, M. Paroncini, "An experimental study of natural convection in a differentially heated cavity through a 2D-PIV system," International Journal of Heat and Mass Transfer, vol. 52, pp. 355-365, 2009.

[15] T.F. Ayinde, S.A.M. Said, M.A. Habib, "Experimental investigation of turbulent natural convection flow in a channel," Heat Mass Transfer, vol. 42, pp. 169-177, 2006.

[16] J.D. Posner, C.R. Buchanan, D. Dunn-Rankin, "Measurement and prediction of indoor air flow in a model room," Energy and Buildings, vol. 35, pp. 515-526, 2003.

[17] C. Sanjuan, M.N. Sanchez, M. del Rosario Heras, E. Blanco, "Experimental analysis of natural convection in open joint ventilated facades with 2D PIV," Building and Environment, vol. 46, pp. 2314-2325, 2011.

[18] C. Sanjuan, M.J. Suarez, E. Blanco, M. del Rosario Heras, "Development and experimental validation of a simulation model for open joint ventilated facades," Energy and Buildings, vol. 43, pp. 3446-3456, 2011.

[19] EN 442-2:1996, Radiators and Convectors – Part 2: Test Methods and Rating, 2003.

[20] Dantec Dynamics, Dynamic Studio v3.31 User's Guide, 2012.

[21] Y.A. Cengel, M.A. Boles, Thermodynamics: An Engineering Approach. McGraw-Hill, 2002.